Comparative Analysis of Image Quality and Radiation Dose in Siemens Single-Source CT, 2nd Generation Dual-Source CT, and 3rd Generation Dual-Source CT Scanners Using PBU 60 Whole Body Phantom

Amit Kumar[1], Monika[2]
[1]*Tutor Technologist, PGIMER, Chandigarh*
[2] *Senior Technologist, PGIMER, Chandigarh*

1.0 Introduction

Computed tomography (CT) has been established as a safe and non-invasive modality. This makes radiation safety pivotal, especially for paediatric and oncological patients, as the latter often undergo multiple CT-examinations in the course of disease surveillance. Many new technologies and approaches have been continuously implemented to reduce the radiation dose, since the introduction of CT in the early 1970's. Important determinants in radiation dose and image quality are detector efficiency, tube potential, tube current, scanned area and usage of post processing denoising technique, such as iterative reconstruction. Decreasing the tube current at a constant tube potential lowers the radiation dose, but simultaneously increases the image noise thus impairing image quality. As the human body is non-homogeneous in terms of tissue density and topologically inconsistent, the trade-off between radiation dose and image quality calls for, applying different dose-reducing techniques, such as automatic tube current modulation [1,2] or choosing a lower tube potential, if the patient's habitus permits [3]. The resulting increased signal-to-noise ratio can be improved by applying the method of iterative reconstruction (IR). Although the vendor specific algorithms evaluation of radiation dose and application of new dose-efficient techniques in whole-body-CT (WBCT) is however still scarce and has been predominantly focused on trauma patient. Acquisitions with two activated tubes at two different voltage settings form the basis for material decomposition [4]. Optimal discrimination between two materials is achieved with a large spectral separation, which can be enhanced by using an additional filtration. The use of tin filtration in the high-kV tube hardens the high energy kV spectrum, resulting in an improved material separation, without affecting the image quality and dose. In order to observe and help standardize CT radiation dose, manufacturers have developed monitoring and tracking software in order to better evaluate the vast amount of data. Consequently, the purpose of this study is to evaluate and compare the radiation dose and image quality of WBCT performed on the 3rd-generation dual-source-CT (DSCT) with 2nd-generation DSCT and 128-slices Single-Source-CT

2.0 Materials and Methods

2.1 This prospective study was approved by the ethical committee of PGIMER, Chandigarh.

2.2 CT machines used for study.

PRODUCT	SOMATOM FORCE	SOMATOM DEFINITION FLASH	SOMATOM AS PLUS
	Siemens Somatom Definition Force	Siemens Somatom Definition Flash	Siemens Somatom Definition AS+
FDA cleared	2014	2009	2008
	Dual Source CT	Dual Source CT	Single Source CT
Gantry	Slip ring	Slip ring	Slip ring
Detector type	2x multislice stellar infinity	2x multislice stellar detector	2x UFC multislice stellar detector
No of rows	192	128	32w/64 channels
Reconstructed slice width option in mm	0.4,0.5,0.6-20	0.4 (optional, with z-UHR), 0.5, 0.6, 0.75, 1, 1.5, 2, 3, 4, 5, 6, 7, 8, 10	0.4 and 0.5 (optional z-UHR), 0.6, 0.75, 1, 1.5, 2, 3, 4, 5, 6, 7, 8, 10
Detector width, mm	52.5	38.4	19.2
Rotation times, sec., 360 degrees	0.25 (optional), 0.285, 0.325 (optional), 0.5, 1 s	0.28 (optional), 0.33, 0.5, 1	0.28, 0.33, 0.5, 1 s
Gantry aperture, cm	78	78	78
X-ray tube anode	2 x VECTRON	2 x STRATON MX P	STRATON MX P
Heat storage, HU	30 MHU (equivalent value compared to the performance of a conventional tube)	0 MHU (0.6 MHU capacity combined with 7.3 MHU/min (5,400 kJ/min) cooling rate is comparable to the performance of a conventional tube with approximately 50 MHU (37,000 kJ) anode heat storage capacity)	0 MHU (0.6 MHU capacity combined with 7.3 MHU/min (5,400 kJ/min) cooling rate is comparable to the performance of a conventional tube with approximately 50 MHU (37,000 kJ) anode heat storage capacity)

2.3 CT Whole Body Phantom PBU-60

Phantom study done for a WBCT performed on the 3rd-generation dual-source-CT (DSCT) with 2nd-generation DSCT and 128-slices Single-Source-CT



Materials of PBU-60.

Soft tissue and Organs	Urethane Base Resin (SZ-50)
Synthetic Bone	Epoxy Base Resin
Joint Attachments	Epoxy, Urethane with Carbon Fiber
Screws	Polycarbonate

HU numbers of each organ

Organs		HU* numbers	Remarks
Soft tissue		8	
Brain	Brain	40	
	Ventricles	10	
	Cerebral artery	280	
Eye balls		20	
Aorta		40	
Vena cava		40	
Trachea	Up to the first bifurcation	−800	Urethane foam
	From the first bifurcation to the small branches	8	Pipe wall's HU number
Heart		40	
Pulmonary vessels		8	Shown up to the forth bifurcations
Costal cartilage		90	
Liver	Liver	70	Incl. the portal vein
	Hepatic veins	40	

Organs		HU* numbers	Remarks
Gall bladder		20	
Pancreas		30	
Spleen		50	
Kidneys	Kidneys	30	
	Renal veins	40	
	Ureters	10	
Ureters		10	
Urinary bladder	Simulated content	10	
	Bladder wall	30	
Seminal vesicle		25	
Prostate		50	
Sigmoid colon wall		70	
Rectum wall		70	

* The Hounsfield numbers shown above are approximate figures of the calculated values and not actual measurement values.

collimation of 128 × 0.6 mm by z-flying focal spot and a pitch of 1.0. Acquisition was performed in the cranio-caudal direction from the vertex to the pelvic floor, Data were reconstructed with 1.5 mm section thickness using the i32f kernel and a strength parameter of 3 for the advanced modeled iterative reconstruction algorithm (ADMIRE).

Examinations on the 2nd-generation 128 slices DSCT (SOMATOM definition Flash, Siemens Healthcare) were also performed with automated tube current modulation in Dual-Energy mode 80- 140 with tin filter and tube current modulation. Although the pitch was set at 1.0, collimation setting and acquisition protocol were identical to the 3rd-generation DSCT. Data were reconstructed with 1.5 mm section thickness using the i30f kernel and a strength parameter of 3 for the sonogram affirmed iterative reconstruction (SAFIRE).

Examinations on the 128-slices SSCT (SOMATOM AS+ Siemens Healthcare) were performed with automated tube current modulation and 80-140 tube voltage. Rotation time was set at 0.5 s with a collimation of 128 × 0.6 mm by z-flying focal spot and a pitch of 1.0. Contrast-media application and acquisition protocols were identical to the previously mentioned. Data were reconstructed with 1.5mm section thickness and i30f kernel by using sonogram affirmed iterative reconstruction (SAFIRE).

3.0 TECHNIQUES

CT-examinations on the 3rd-generation 192 slices DSCT (SOMATOM Force, Siemens Healthcare) were performed with automated tube current modulation in Dual-Energy mode 80-150, with tin filtration, automated tube current modulation (care Dose 4D, Siemens Healthcare), [7] rotation time of 0.5 s,

PARAMETRES	S S C T	D S C T 2 ND GEN.	D S C T 3 RD GEN.
TUBE VOLTAGE(KVP)	80/140	80/140 sn	80/150s n
REFERENCE TUBE CURRENT	220	200	150
PITCH	1	1	1
ROTATION TIME	0.5	0.5	0.5
COLLIMATION	128x0.6	128x0.6	128x0.6
CTDI (VOL)	3.032	2.85	1.69
D L P	305.4	276	167.4
ALGORITHM	saffire	saffire	admire
STRENGTH LEVEL	1	3	3
SLICE THICKNESS	1.5	1.5	1.5
SLICE INTERVAL	1.5	1.5	1.5
RECONSTRUCTION KERNELS	i30 f	i30f	i32
LINEAR BLENDING IN D S C T	50-50	50-50	50-50
TIN FILTER	no	sn	sn
fov	400	400	400

3.1 BLENDING

In dual-energy CT (DECT) scans, "blending" refers to the process of combining images acquired at two different energy levels (typically low and high kVp) to create a single image that simulates a standard single-energy CT image. This technique helps in enhancing image quality and improving diagnostic accuracy. Here are some key points about blending in (DECT)12: Image Combination: Blended images are created by combining low-energy (e.g., 80 kVp) and high-energy (e.g., 140 kVp) data. This combination helps to simulate a standard 120 kVp dataset, which is commonly used in single-energy CT scans.

LINEAR AND NONLINEAR BLENDING

LINEAR BLENDING Linear blending combines images from low and high energy scans in a straightforward, additive manner. This method is often used to create images that simulate a standard single-energy CT scan. It helps in maintaining a balance between image quality and noise reduction. Simplicity and ease of implementation. It provides a good balance of contrast and noise.

Nonlinear Blending Nonlinear blending uses more complex algorithms to combine the images, taking into account the nonlinear relationships between different tissue types and their attenuation at different energy levels.[8] This method can enhance specific features or materials within the body, such as differentiating between types of tissues or highlighting contrast agents more effectively. Improved contrast and differentiation of materials. It can provide better diagnostic information by enhancing specific features that are not as easily distinguishable with linear blending [9].

Comparison Image Quality: Nonlinear blending generally provides better image quality and material differentiation compared to linear blending.

Use Cases: Linear blending is suitable for general imaging purposes, while nonlinear blending is preferred for specific diagnostic tasks where enhanced material differentiation is required.

Material Differentiation: DECT allows for material decomposition, which means it can differentiate between different types of tissues or substances based on their attenuation properties at different energy levels. This is particularly useful for identifying materials like iodine, calcium, and uric acid.

Virtual Monochromatic Imaging: DECT can generate virtual monochromatic images at different energy levels, which can enhance contrast and improve the visualization of lesions.1

Clinical Applications: Blended images are used in various clinical applications, including emergency medicine, radiation therapy, and routine diagnostic imaging. They help in better visualization of contrast-

enhanced lesions and improve the detectability of diseases [10].

3.2 CARE Dose4D CARE Dose4D performs automatic tube-current modulation in the angular and longitudinal directions and also adapts to different anatomical regions and patient sizes.

4. Image quality

4.1. Objective image quality

Signal-to-noise ratio (SNR) and the contrast-to-noise ratio (CNR) they were assessed by placing an area of interest (ROI) of ~0.5cm^2 in the tissue and background at three different z-levels and measuring the mean density and the standard deviation in Hounsfield unit (HU). Reference ROIs were placed in the subcutaneous adipose tissue at the same level. CNR and SNR were calculated according to [11]:

CNR = HU (tissue) – HU (back ground tissue)/ mean standard deviation

SNR = HU (tissue)/ mean standard deviation

4.2 Subjective image quality

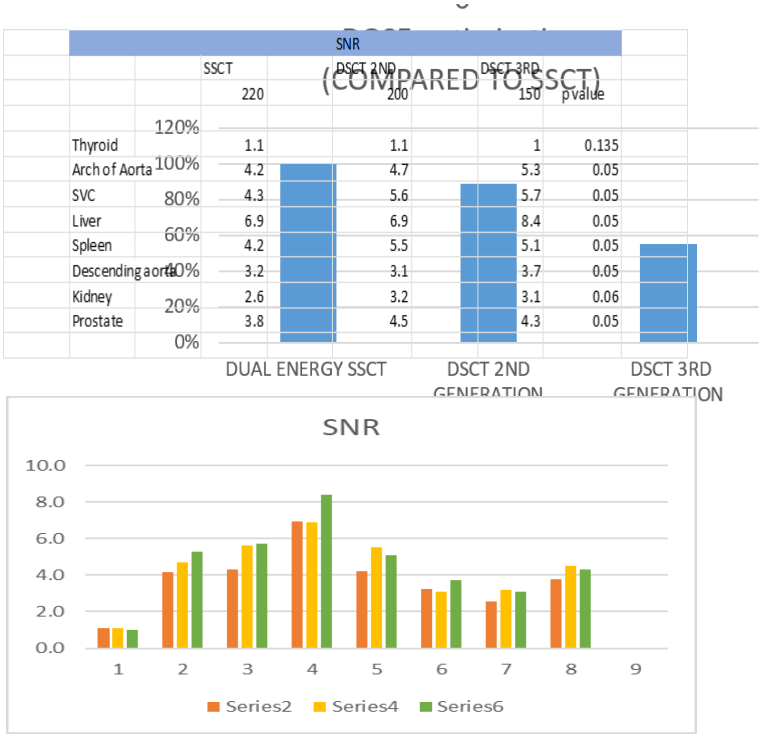
Solid organs such as adrenal glands and lymph nodes are important markers for CT-surveillance studies. Those structures have been chosen for subjective image quality evaluation. Lymph nodes were evaluated at the level of the mediastinum, axilla, and lung hilum. Evaluation was completed by two radiologists with >3 years and >10 years of clinical experience in WBCT on a clinically approved radiology-workstation with a soft-tissue window setting of 400/50 (width/center). Any discrepancy was solved by consensus. An alternated version of the European Guidelines on Quality Criteria for Computed Tomography with a 5-point Likert scale was applied [12]: 5. Excellent image quality with excellent delineation, no blurriness, and fully diagnostic; 4. Good image quality with good delineation, slight blurriness, and fully diagnostic; 3.Acceptable image quality with acceptable delineation or blurriness, but diagnostically still usable; 2. Insufficient image quality with on-definable delineation or blurriness and not recommended for diagnostic usage. 1. Non-usable image quality.

4.3. Radiation dose

CTDI-vol

computed tomography (CT) scanners display a value called CT dose index-volume (CTDI-vol), in units of milli-gray (mGy). CTDI-vol is calculated by the scanner based on the radiation output for the particular scan. Since most modern scanners automatically adjust output based on the size and density of the patient, this will vary patient to patient. The CTDI-vol is based on the radiation dose which would be absorbed by a specific size phantom, either 16 or 32 cm. It is not the dose to the specific patient, but it is meant to be a comparison metric for different scans or scanners. Accreditation requires sites to measure the accuracy of the calculated CTDI-vol, by actually measuring it with an ion chamber and phantom.

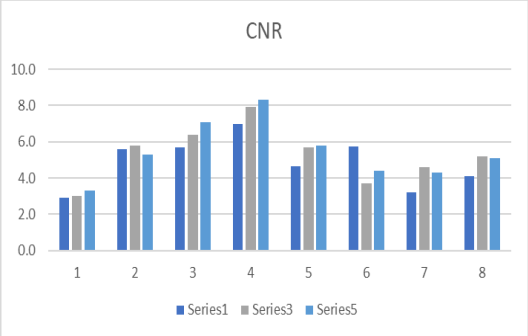
DLP The dose-linear product (DLP) is calculated by multiplying the CTDI-vol, which is given for a centimeter (cm), by the number of centimeters scanned. It is given in units of mGy-cm



DATA ANALYSIS

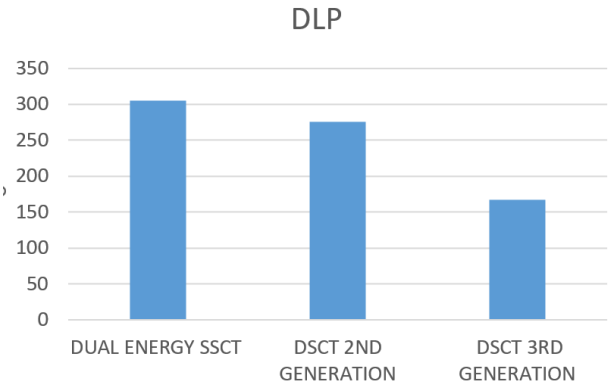
The present study uses SPSS for inferential data analysis. Non-parametric test is employed to calculate the statistical difference between the readings of the three CT generation machines. Friedman test used at 95% confidence interval to employ the results. P-value less than 0.05 is considered as significant. For descriptive data analysis and data interpretation through bar charts, MS Excel is used.

RESULTS



CTDI (VOL)	3.032
D L P	305.4

After evaluation it was found that with consistent image quality at similar CNR, SNR values and subjectively at Likert scale 4.0 to 4.7. same image quality, radiation doses were found to be decreasing with each generation of CT. Radiation dose was less in Second gen CT and third gen CT by 11% and 45% respectively compared to first generation CT scanner.



DISCUSSION

This study was done on 3 different machines using different parameters of reference mA from 150 to 220, keeping other parameters consistent between all the scanners.

	CNR			
	SSCT	DSCT 2ND	DSCT 3RD	
	220	200	150	p value
Thyroid	2.9	3	3.3	0.05
Arch of Aorta	5.6	5.8	5.3	0.09
SVC	5.7	6.4	7.1	0.05
Liver	7.0	7.9	8.3	0.05
Spleen	4.7	5.7	5.8	0.09
Descending aorta	5.7	3.7	4.4	0.05
Kidney	3.2	4.6	4.3	0.06
Prostate	4.1	5.2	5.1	0.05

kVp for dual energy sources were kept at 80 and 140. 80 and 150 in dual source third generation. Linear blending of 50%-50% were performed so as to get single dataset for comparison. Parameters such as CNR and SNR were assessed at 8 different ROI ranging from neck region to prostate region at solid organs and vasculature. Thyroid, SVC, arch of aorta, liver, spleen, descending aorta, left kidney and prostate were evaluated and compared with each other. ROI size was kept consistent at 5 mm^2. Subjective and objective reading were assessed at consistent image quality at similar CNR, SNR values and subjectively at Likert scale 4.0 to 4.7. Radiation doses as provided by CT scanners were compared and compared later. After evaluation it was found that with same image quality, radiation doses were found to be decreasing with each generation of CT. Radiation dose was less in Second gen CT and third gen CT by 11% and 45% respectively compared to first generation CT scanner.

In this study we demonstrate the evolution of CT-technology over three generations in respect to radiation dose and image quality, indicating that the implementation of new technologies such as new detectors, tin filter and reconstruction algorithms helps in reducing the radiation exposure without compromising the image quality. Newer detector types, new filters and reconstruction techniques can be

attributed for this reduction of radiation doses between the 3 generation of scanners.

CONCLUSION

In this study we demonstrate the evolution of CT-technology over three generations in respect to radiation dose and image quality, indicating that the implementation of new technologies such as new detectors and reconstruction algorithms helps in reducing the radiation exposure without compromising the image quality.

These findings are especially important for pediatric, cardiac, young females and oncological patients, as the cumulative radiation dose accrued especially during repeated follow-up examinations might increase the risk of secondary cancer.

References

[1] M.K. Kalra, M.M. Maher, T.L. Toth, B. Schmidt, B.L. Westerman, H.T. Morgan, S. Saini, Techniques and applications of automatic tube current modulation for CT, Radiology 233 (3) (2004) 649–657.

[2] S. Rizzo, M. Kalra, B. Schmidt, T. Dalal, C. Suess, T. Flohr, M. Blake, S. Saini, Comparison of angular and combined automatic tube current modulation techniques with constant tube current CT of the abdomen and pelvis, AJR Am. J. Roentgenol. 186 (3) (2006) 673–679.

[3] W. Huda, Radiation doses and risks in chest computed tomography examinations, Proc. Am. Thorac. Soc. 4 (4) (2007) 316–320.

[4] T.R. Johnson, B. Krauss, M. Sedlmair, M. Grasruck, H. Bruder, D. Morhard, C. Fink, S. Weckbach, M. Lenhard, B. Schmidt, T. Flohr, M.F. Reiser, C.R. Becker, Material differentiation by dual energy CT: initial experience, Eur. Radiol. 17 (6) (2007) 1510–1517

[5]https://www.kyotokagaku.com/en/products_data/ph-2b/

[6] https://s3.amazonaws.com/sgcimages/36_37_40_41_ITN1115_Siemens.pdf

[7] https://www.mayo.edu/research/documents/care-dose-4d-ct-automatic-exposure-control-system/doc-20086815

[8] Holmes DR 3rd, Fletcher JG, Apel A, Huprich JE, Siddiki H, Hough DM, Schmidt B, Flohr TG, Robb R, McCollough C, Wittmer M, Eusemann C. Evaluation of non-linear blending in dual-energy computed tomography. Eur J Radiol. 2008 Dec;68(3):409-13.

[9] Li S, Wang C, Jiang X, Xu G. Effects of dual-energy CT with non-linear blending on abdominal CT angiography. Korean J Radiol. 2014 Jul-Aug;15(4):430-8. doi: 10.3348/kjr.2014.15.4.430. Epub 2014 Jul 9.

[10] Tatsugami, F., Higaki, T., Nakamura, Y. et al. Dual-energy CT: minimal essentials for radiologists. Jpn J Radiol 40, 547–559 (2022).

[11] F. Bamberg, R. Marcus, W. Sommer, F. Schwarz, K. Nikolaou, C.R. Becker, M.F. Reiser, T.R. Johnson, Diagnostic image quality of a comprehensive high-pitch dual-spiral cardiothoracic CT protocol in patients with undifferentiated acute chest pain, Eur. J. Radiol. 81 (12) (2012) 3697–3702.

[12] S.J.G.G. Bongartz, A.G. Jurik, M. Leonardi, E. van Persijn, van Meerten, R. Rodríguez, K. Schneider, A. Calzado, J. Geleijns, K.A. Jessen, W. Panzer, P.C. Shrimpton, G. Tosi, European Guidelines for Multislice Computed Tomography, 2004

films with biaxial anisotropy,‖in*Proc.1987INTERMAG Conf.*, 1987,pp. 2.2-1-2.2-6.

(Presented ConferencePaperstyle)

[11] G. W. Juette and L. E. Zeffanella, ―Radionoisecurrentsn short sections onbundleconductors,‖presentedattheIEEESummerPower Meeting,Dallas,TX,June 22-27,1990.

(ThesisorDissertation style)

[12] J.Williams,―Narrow-bandanalyzer,‖Ph.D.dissertation,Dept.Elect.Eng., Harvard Univ.,Cambridge, MA,1993.

[13] N. Kawasaki, ―Parametric study of thermal and chemical nonequilibriumnozzle flow,‖ M.S.

thesis,Dept.Electron.Eng.,OsakaUniv., Osaka,Japan, 1993.

(Patent style)

[14] J.P.Wilkinson,-Nonlinear resonantcircuitdevices,‖ U.S.Patent3624 12,July16, 1990.

(Standards style)

[15] *LetterSymbolsforQuantities,*ANSI StandardY10.5-1968.

(Handbookstyle)

[16] *TransmissionSystemsforCommunications*,3rded., WesternElectricCo.,Winston-Salem,NC,1985, pp. 44-60.

[17] *Motorola Semiconductor Data Manual*, Motorola SemiconductorProducts Inc.,Phoenix,AZ, 1989.

(JournalOnline Sourcesstyle)

[18] R.J.Vidmar.(August1992).Ontheuseofatmospheri cplasmasas electromagneticreflectors.*IEEETrans.PlasmaSci.* [Online].21(3).pp. 876-880. Available:http://www.halcyon.com/pub/journals/ 21ps03-vidmar